ACADEMIA ROMÂNĂ
Revue Roumaine de Chimie
http://web.icf.ro/rrch/

Rev. Roum. Chim.,
2021, *66*(6), 493–507
DOI: 10.33224/rrch.2021.66.6.02

CONSTRUCTION OF MODIFIED NANOTUBE CARBON CARBOXYL BY NEW METHOD AND APPLICATION IN DISPERSIVE SOLID PHASE EXTRACTION FOR PRECONCENTRATION OF Ni^{2+}

Ali MOGHIMI,[a,*] Milad ABNIKI[b], Mehdi KHALAJ[c] and Mahnaz QOMI[d]

[a]Department of Chemistry, Varamin-Pishva Branch, Islamic Azad University, Varamin, Iran
[b]Department of Resin and Additives, Institute for Color Science and Technology, Tehran, Iran
[c]Department of Chemistry, Buinzahra Branch, Islamic Azad University, Buinzahra, Iran
[d]Department of Medicinal Chemistry, Faculty of pharmaceutical chemistry, Pharmaceutical science branch, Islamic Azad University, Tehran, Iran

Received August 12, 2020

Applying a facile and accessible sample preparation method is highly important before the experimental analysis process. In the current study, a technique was introduced for preconcentration and analysis of trace amounts of Ni (II) ions in water samples. The important parameters in the analytical procedure of Ni (II) ions were optimized such as the pH of extraction, amount and type of elution solvent, time of extraction, and the effect of another ion. Freundlich, Langmuir, Temkin, and Dubinin–Radushkevich isotherm models were used to estimate the adsorption mode of Ni (II) ions by a nanotube carbon carboxyl. The Freundlich model was achieved for Ni (II) ions adsorption from the isotherm studies. The kinetic studies indicating adsorption of Ni (II) ions by nanotube carbon carboxyl were fitted with the pseudo-second-order model, which resulting the chemisorption mode is the rate-limiting process for the Ni (II) adsorption. Analytical parameters such as the concentration factor, the limit of detection (LOD) of the technique, and relative standard deviation (RSD %) were achieved as 20.8, 6 µg L-1, and 1.35%, respectively.

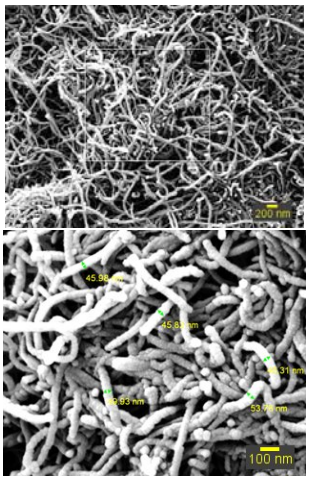

INTRODUCTION

Heavy metals increase the risk of cancer, renal toxicity, and raised tumor growth. The US Environment Protection Agency (US-EPA) has categorized it as one of the B1 group carcinogenic elements.[1] Widespread use of heavy metals in the plating industry, pesticide manufacturing, battery technologies, and the paper industry has increased the risk of human exposure. Heavy metals are discharged into the wastewater at all stages of the production cycle. Discharge occurs during metal extraction, product production, use, and disposal. Most of the heavy metals enter the biological cycle either directly or indirectly through industrial wastewater and enter the soil, and then these heavy metals collected in the soil are washed into groundwater reservoirs. Heavy metals studied in terms of high risk include nickel, copper, arsenic, chromium, lead and mercury, cadmium.[2,3] Among the various pollutants, nickel is considered an important ion water pollution is a concern. Nickel ions as heavy metal ions are commonly found in various industrial effluents such as metal alloys,

* Corresponding author: kamran9537@yahoo.com; alimoghimi@iauvaramin.ac.ir

alloys, paints, non-ferrous metals, power plants, stainless steel, and if the industrial effluents containing these ions are not treated properly, they can enter the environment and Groundwater. The maximum allowable total nickel in drinking water has been set at a concentration of 0.02 mg/L by the World Health Organization (WHO). Complications of high concentrations of nickel ions can include nausea, vomiting, diarrhea, chest pain, shortness of breath, and more.[4,5]

The direct designation of nickel in aqueous samples by flame atomic absorption spectrometry (FAAS) is very difficult because of the slight concentration of nickel metal ions and likewise interfering influences of the matrix components. Consequently, separation and preconcentration stages are often required to obtain accurate, sensitive, and reliable consequences by FAAS. Several procedures including precipitation/co-precipitation,[6] and liquid-liquid,[7-9] cloud point,[10] solid-phase extraction[11] (SPE) have been developed for the separation and preconcentration of trace nickel. Among the related methods, solid-phase extraction is the most common technique applied for preconcentration of an analyte in environmental aqueous because of its benefits of high enrichment factor, great recovery value, rapid phase separation, cost-effective, low usage of organic solvents and its ability to be combined with different detection paths in the on-line or off-line mode forms.[11-13] Recently, a new type of SPE, magnetic solid-phase extraction (MSPE) has been used by several researchers. The MSPE is based on magnetic materials as sorbent, which can be isolated from the matrix quickly by using a magnet. Compared to other isolation methods, MSPE can improve extraction efficiency and can simplify the preprocessing. Furthermore, the application of nanomaterials such as activated carbon,[14] different methods, co-extractant ligands has involved significant attention.[15,16]

Solid-phase extraction (SPE) or in other words the liquid-solid extraction is a famous and growing technique for sample preparation and measurement. Yet, the disks modified ligand as a selective approach to separate and pre-concentrate heavy metals in aqueous samples.[17-26] Over the recent investigations,[27-29] the determinate depends on the esterase activity of a DNA-linked ions complex. For optimizing the system and exploring the structure-activity relationships, a sensitive probe would be beneficial to permit direct detection of esterase activity of ion-ligand in low concentrations. The chelated ions were desorbed and identified by GF-AAS. The modified solid-phase could be applied at least 50 times with appropriate reproducibility without any variation in the composition of the adsorbent, magnetic nano-Fe_3O_4 chitosan/graphene oxide. Consequently, in the current investigation, the researchers focused on the first application of MWCNTs-COOH as a novel adsorbent for dispersive solid-phase and extraction of Ni^{2+} wastewater samples before the spectrofluorometric determination at GF-AAS after excitation.

EXPERIMENTAL

Instrumentation

The determination of Ni^{2+} by PG-990flame atomic absorption spectrometer is equipped with HI-HCl which was done according to the recommendations of the manufacturers. Accordingly, the pH measurements were used by Sartorius model PB-11.

Materials

In the current investigation, the following materials have been applied for the experiments; functionalized carbon nanotubes with carboxyl, hexahydrate Ni (II) nitrate, thio-semi-carbazide ligand, buffer, and nitric acid. Additionally, ethylenediamine, thio-semi-carbazide ligand (CH_5N_3S) was prepared from Darmstadt, Germany of Merck.

Synthesis of carboxylic functionalized carbon nanotubes

A mixture of 4.0 g of nanotubes and 100 mL of HNO_3 was refluxed under stirring conditions at 120°C. The product of (MWCNTs-COOH) was filtered with 1.2 mcm filter paper and then washed with deionized water to obtain the neutral pH. Finally, it was inserted in the oven at 60°C to dry off completely.[30]

Synthesis of amine-functionalized carbon nanotubes

A certain amount of product produced in the previous step (MWCNTs-COOH) was added to 20 mL of ethylenediamine solution and then, it was placed in an ultrasonic bath for 5 h. In the last step, it was stirred for 24 h at 60 °C and finally, the product was collected by filtration and washed with methanol and dried in a vacuum oven.[31]

The initial experiment of Ni^{2+} extraction for determining the suitable adsorbent

The procedure for extraction and recovery of Ni ions by MWCNTs-COOH is as follows; in the first step, 0.2 g of thiosemicarbazone ligand and 0.3 g of MWCNTs (carboxylic and amine functions) and were dissolved in the little amount of acetone, and then it dried. Four 50-mL ballons were adopted, and then 0.05 g of MWCNT (amine function) was poured into one of the balloons. Afterward, 0.05 g MWCNT with carboxylic function, 0.05 g combination of ligand and amine MWCNT, and 0.05 g mixture of ligand and carboxylic MWCNT were added to each other balloons. Thereupon, a 1 mL buffer solution with a pH of 4.5 was added to balloons and a 2 ppm solution was prepared with an analyte. Four solutions were shaken at 25°C for 20 min, then these solutions

for 15 min were centrifuged and the supernatant injected into an atomic absorption apparatus.

The effect of adsorbent amount for Ni^{2+} extraction

Seven 2.0 ppm solutions with 50 mL of Ni^{2+} were provided and poured into seven flasks. Seven solutions were adjusted at pH=10 (optimum pH) and different amounts of the adsorbent (0.005, 0.01, 0.03, 0.05, 0.07, 0.12, and 0.15) added to flasks. The mixtures were shaken for 20 min, and then the mixtures were centrifuged and the top solution of the examine tube injected in flame atomic absorption spectrophotometry.

Adsorption isotherms

In this study, Langmuir, Freundlich, Temkin, Dubinin–Radushkevich isotherms were studied to explain the Ni^{2+} adsorption mechanism. The Langmuir isotherm considers that the maximum sorption happens by the formation of a monolayer onto the surface as homogeneous, without any interaction between the adsorbent.[32,33] The Langmuir model is given by the below relationship.

$$\frac{c_e}{q_e} = \frac{c_e}{q_m} + \frac{1}{q_m K_L} \quad (1)$$

where the q_e is the amount of sorbed of the Ni^{2+} on the surface of MWCNT (mg g^{-1}) at equilibrium, the term of C_e is the concentration of Ni^{2+} in the mixture at equilibrium (mg L^{-1}), the q_m (mg g^{-1}) is the maximum sorption capacity of the MWCNT, and K_L (L mg^{-1}) is Langmuir isotherm constant and attributed to the sorption energy.[34]

$$R_L = \frac{1}{1 + (K_L c_0)} \quad (2)$$

In relation (2), C_0 is the maximum primary Ni^{2+} concentration. The R_L values ascertain the type of adsorption to be linear ($R_L = 1$), unfavorable ($R_L > 1$), favorable ($0 < R_L < 1$), and irreversible ($R_L = 0$).

The Freundlich model is expressed as an experimental type and is used commonly for a heterogeneous surface.[35] A type of the Freundlich isotherm is calculated from the below relation:

$$\ln q_e = \ln K_F + \frac{1}{n} \ln c_e \quad (3)$$

In relation (3), K_F is attributed to the isotherm constant and n the sorption intensity. According to the studies, desirable adsorption should be a value of 1/n between 0.1 and 1.[36]

The Temkin model supposes that the sorption energy decreases when increasing the adsorbate places occupied by Ni^{2+}.

$$q_e = \frac{RT}{b} \ln A + \frac{RT}{b} \ln c_e \quad (4)$$

$$B = \frac{RT}{b} \quad (5)$$

where T is the absolute temperature (K), R is the universal gas constant (8.314 J mol^{-1} K^{-1}), b is the isotherm constant, A and B are Temkin constants and is an index of sorption heat (J mol^{-1}), and isotherm binding equilibrium constant (L g^{-1}), respectively.

The isotherms mentioned above do not provide any idea about the metal adsorption mechanism. Dubinin–Radushkevich isotherm was applied to understand the Ni^{2+} adsorption type. This model is an empirical isotherm form and it is expressed the Gaussian energy distribution from adsorbate adsorption mechanism onto a heterogeneous surface and linear model is given as:[37]

$$\ln q_e = \ln q_D - B_D (\ln RT(1 + 1/C_e))^2 \quad (6)$$

where, B_D is attributed to the free energy of adsorption per mole of the adsorbate as it moves to the surface of the biomass from unlimited distance in the mixture ($mol^2.J^2$), q_D is Dubinin–Radushkevich constant, R is the universal gas constant (8.314 J mol^{-1} K^{-1}), T is the absolute temperature (K).

The E ($J \cdot mol^{-1}$) is the value of activation energy that is used to determine the type of physical and chemical sorption process. Also, the value of E was necessary energy for eliminating a molecule of adsorbate from its location in the adsorption site to the infinity and defined by the following relationship:

$$E = [1/\sqrt{2B_{DR}}] \quad (7)$$

Adsorption kinetics

To study the adsorption mechanism of Ni^{2+}ions onto the MWCNT, three models of simple kinetic including pseudo-first and second-order and intraparticle diffusion were used to fit the adsorption time data achieved. The pseudo-first-order model is expressed as shown in Eq. 7:[38]

$$\log(q_e - q_t) = \log q_e - \frac{k_1 t}{2.303} \quad (8)$$

The pseudo-second-order kinetic model[39] is written as follows:

$$\frac{t}{q_t} = \frac{1}{k_2 q_e^2} + \frac{1}{q_e} t \quad (9)$$

In equations (8, 9) k_1 and k_2 express the pseudo-first and second-order rate constants, in min^{-1} and g mg^{-1} min^{-1}, respectively; q_e and qt are the adsorption uptake in equilibrium ($t = \infty$) and adsorption uptake (t), in (mg g^{-1}), respectively. The kinetic obtain results were investigated in the intra-particle diffusion model[40] to the explanation of the diffusion mechanism. This model is written as follows:

$$q_t = k_p t^{1/2} + C \quad (10)$$

k_p is the rate constant of intra-particle diffusion, in mg g^{-1} $min^{1/2}$, and C is a constant attributed to the width of the boundary layer, in mg g^{-1}.

Application on real samples

Once the extraction method was performed by the adsorbent, optimal conditions were achieved for it, and multiple real aqueous samples were investigated. The real samples were as follows; well and drinking water in Pishva Town were collected with temperatures of 20 and 22°C, pH=7.1, 7.3 in 23.8.95 at 9:45, 10:00, respectively. Finally, a fish farming sample was collected at, pH=6.20 in 23.8.95 at 11:20. First, these suitable bottles were provided for the sampling of samples. The bottles were washed first with ordinary and distilled water. The bottles dried completely, and the ‘suitable’ label was attached to each bottle. To collecting

of water samples, the used containers sample dried and cleaned and they had already been washed. For the analysis of the samples in the first stage, colloidal and suspended particles were removed. To this aim, the water samples passed through 0.22 µm filters. Next, the volume of 100 mL of samples was poured into the sample container. The pH of samples was adjusted at 10 and then, nanotube and ligand were added to samples. They stirred for 20 min and the mixture was then centrifuged. Then, they were washed with HNO_3 0.1 M and were shaken again for 20 min. Finally, following the centrifugation of the mixture, absorption of Ni ion was identified from the filtered solution by flame atomic absorption spectrophotometry. In the first step, the sample itself was injected into the apparatus without any Ni ion, wherein water samples, the device displayed no absorption. To identify certain amounts of Ni of the samples, the method of standard elevation was used. This stage was accomplished like the first step, the only discrepancy was that 0.5 mL of 200 ppm solution with Ni^{2+} added to the water samples. Finally, the absorption of Ni ion was identified from the filtered solution by flame atomic absorption spectrophotometry.

RESULT AND DISCUSSION

This section deals with the results of the research experiments. The results achieved in the experimental chapter, calibration curve, and the factors influencing the extraction (*e.g.* pH, temperature effect, time, etc.) of Ni^{2+} ion by the MWCNTs are discussed which are followed in the presentation of scientific justification and overall conclusion of the study.

The tests conducted to confirm the nanotubes functionalized with carboxyl

The FTIR spectrum of the compound in Figs. 1, 2 displays two vibration bands at 1107.78 cm^{-1} is ascribed to the C-O bond depending on the carbon attached to the carboxylic group. Besides, the peak at 1593.65 cm^{-1} is associated with C=O bond of the carboxylic group. Finally, the broad bands at 3384.12 cm^{-1} attributed to the stretching vibration of O-H bond.[41] The dominant bands at 1593.65 and 1105.37 cm^{-1} can be indexed to the carboxylic groups on the carbon nanotubes.

Investigation of the data obtained from the XRD spectrum

Here, to determine the size of MWCNT, the Sherer equation used, which is as follows:

$$D_{(hkl)} = \frac{k\lambda}{\beta_{(hkl)} \cos\theta} \quad (11)$$

D: the mean size of the crystallite (nm), k: the Sherr constant, λ: the wavelength of the tube generating x-ray (nm), β: the peak breadth, θ: diffraction angle.[42]

The following figure illustrates the diffraction of MWCNT-COOH, where peak diffraction of θ=26.5 is clear. In the XRD spectrum, the seen peak is in full congruence with the diffraction peaks associated with the nanotube compound phase. A short band expects when the carboxyl nanotube is functionalized. The diffraction of peak (θ = 26.5) in the XRD pattern is a good indication of the placement of carboxyl groups in the MWCNT[43,44] (Fig. 3).

In the XRD pattern below this compound, there is a reflection peak with a high intensity corresponding to carboxylic nanotube in the area 2θ=26° and a weak peak at 2θ=42.89° that has very sharp and short peaks, respectively (Fig. 4 and Fig. 5).

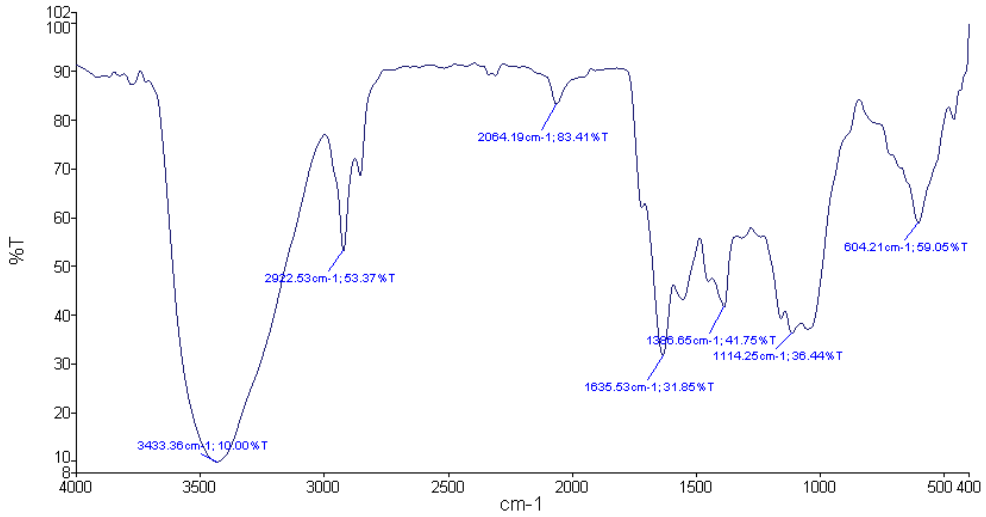

Fig. 1 – FT-IR spectrum of the adsorbent before the adsorption Ni (II).

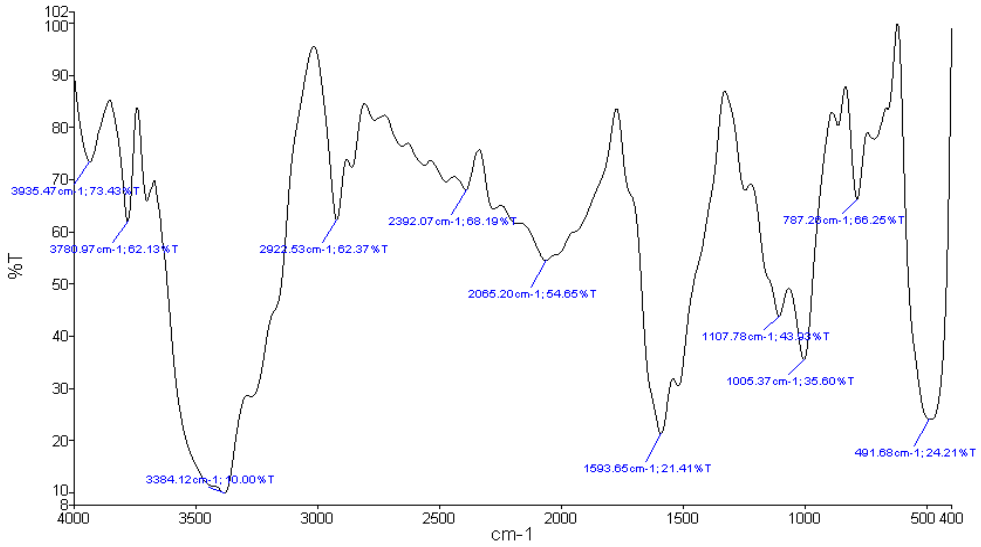

Fig. 2 – FT-IR spectrum of the adsorbent after the adsorption Ni (II).

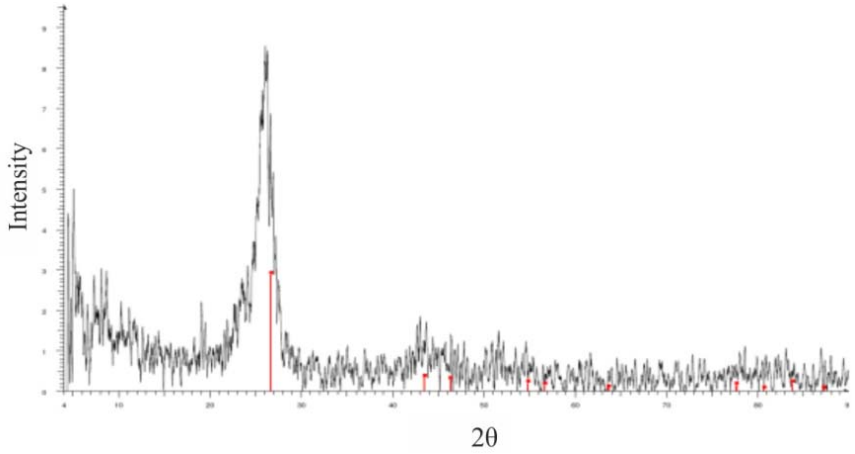

Fig. 3 – XRD images of the carbon nanotubes before the adsorption.

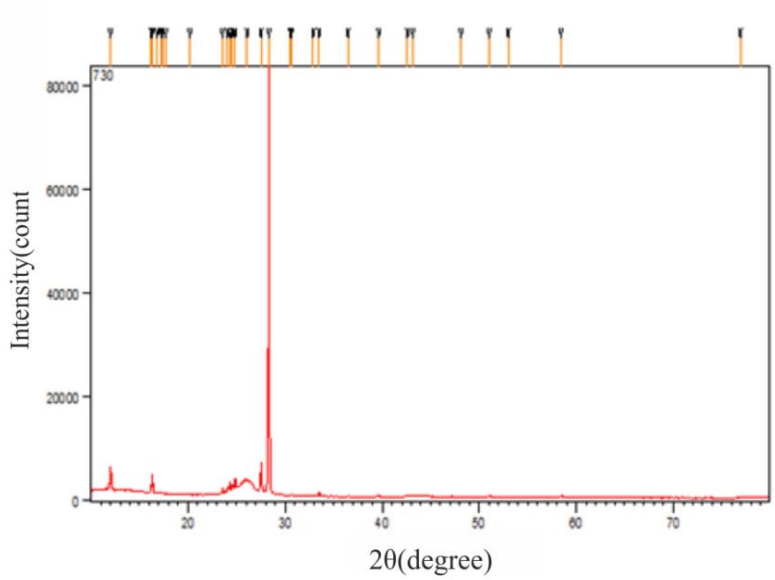

Fig. 4 – XRD images of the adsorbent plus ligand before the adsorption.

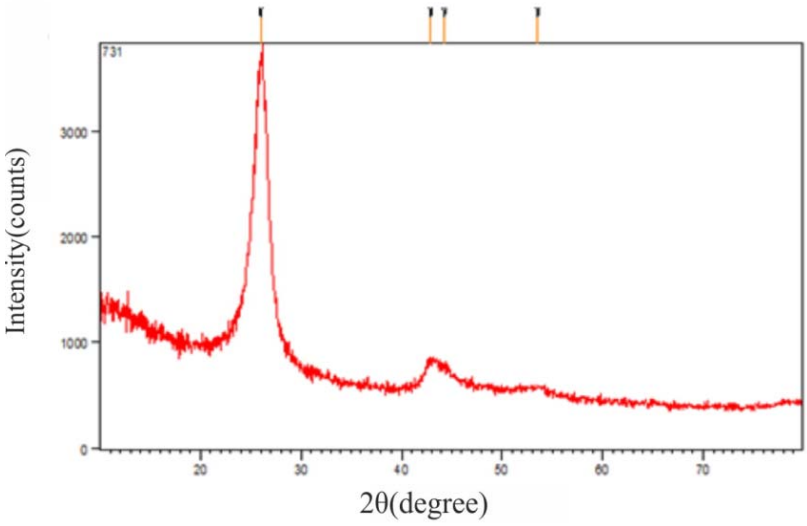

Fig. 5– XRD images of the adsorbent plus ligand after the adsorption.

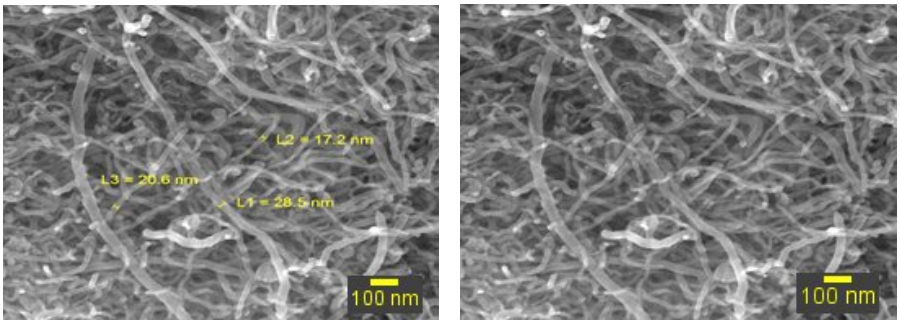

Fig. 6 – SEM correspond to the carbon nanotubes before the adsorption ligand.

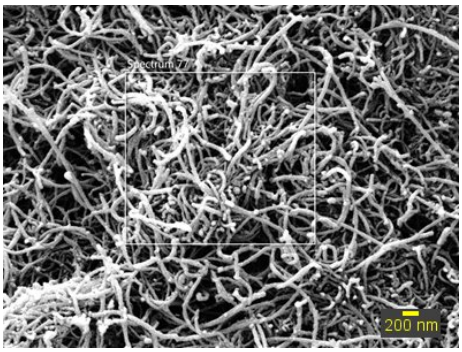

Fig. 7 – SEM image of carbon nanotubes added ligand before the adsorption Ni^{2+}.

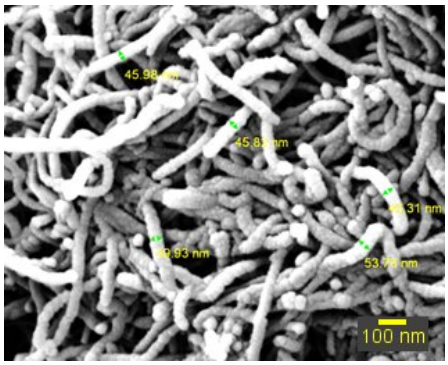

Fig. 8 – SEM of the carbon nanotubes after the adsorption Ni^{2+}.

The following figures reveal the SEM image of MWCNT-COOH. For the MWCNT-COOH, the size of particles achieved as 200 nm Figs. 6, 7.

Furthermore, post-adsorption in Figure 8 of the SEM image shows the deposition of the Ni^{2+} of interest on the MWCNT-COOH. Based on the above figures, it can result that the thickness of planes has been increased. As can be seen in Figure 8, the carboxylic functional group on the surface of MWCNT can be seen as lighter points.

Investigation of the influential factors on Ni^{2+} extraction

Study the effect of pH on Ni^{2+} extraction

The results of this study are provided in Fig. 9. As the results in Fig. 9 indicate, at pH=10, Ni adsorption was maximized, while at lowest and highest pHs, the extent of adsorption declines, inferring that at pH<10 adsorptions of Ni^{2+} ions cannot occur completely. As revealed in Fig. 9, to determine the amount of MWCNTs-COOH required for effective removal of Ni^{2+}, different amounts of the MWCNTs-COOH (50 mg) for modification of MWCNTs-COOH with fixes amount (3 mg) and its effect for the removal of Ni^{2+} from 20 mL solutions of Nickle ion (50 μg/L) were investigated.

Study the effect of MWCNTs-COOH level for Ni^{2+} extraction

The results of this study are shown in Fig. 10. As the results in the table ascertain, at 0.05 g of the MWCNTs-COOH, the adsorption percentage and recovery of Ni^{2+} have been maximized. As Fig. 10 shows, by increasing the adsorbent, the remaining quantity of Ni^{2+} decreases. Fig. 10 shows the amount of remaining Nickle.

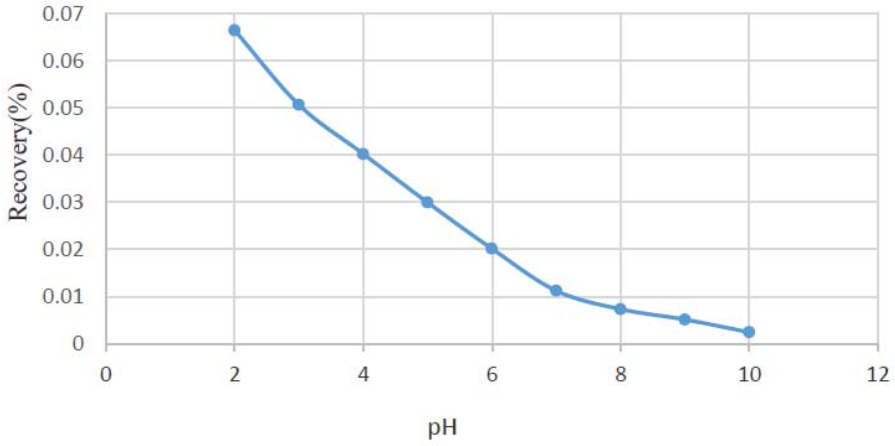

Fig. 9 – The effect of pH in the Ni^{2+} adsorption.

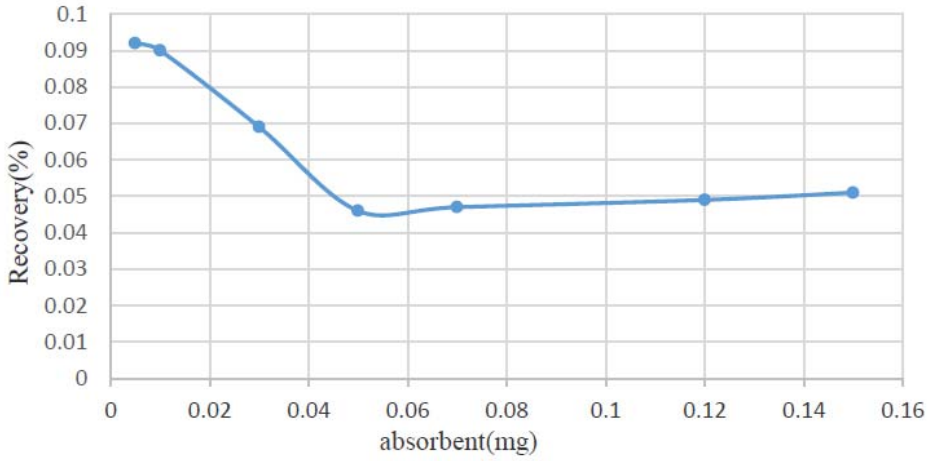

Fig. 10 – The effect of adsorption Ni^{2+} of the adsorbent.

Investigation of the effect of time on Ni^{2+} extraction

The results of this study have been shown in Fig. 11. Based on the results, the extent of absorption increases, and the Ni ions present in the solution find more chance to be adsorbed in the adsorbent's sites. Therefore, the quantitative extraction of Ni ion is possible for a period of longer than 20 min, and within durations longer than 20 min and more, the reaction happens completely.

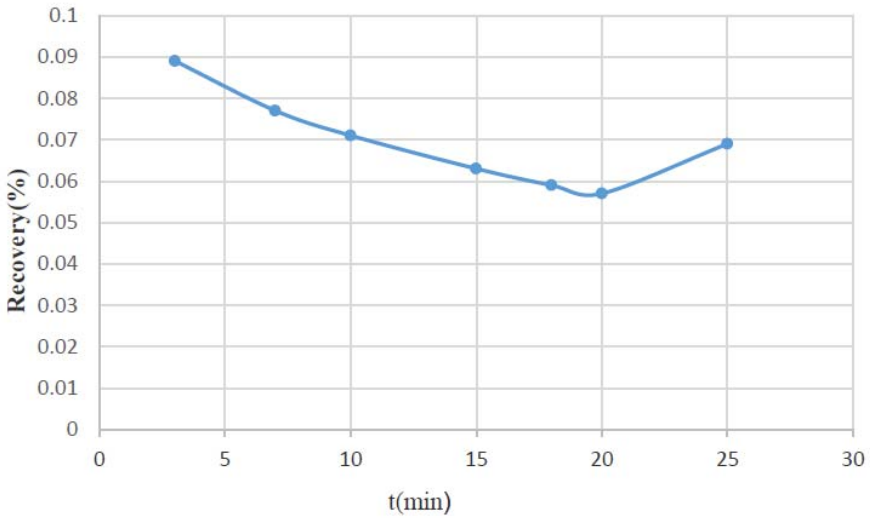

Fig. 11 – The recovery percentage of extraction time Ni^{2+}.

Table 1

Selection of the appropriate desorption for recovery of Ni^{2+}

Solvent	(%) Recovery
HNO_3 0.1M	[a](0.2)90.40
HNO_3 1M	(0.5)85.22
$HNO_3$3M	(0.2)79.65
H_2SO_4 0.1M	(0.5)72.62
$H_2SO_4$1M	(0.3)73.70
NaOH0.1 M	(0.2)68.46

[a] measurement RSD after three replications

Survey of the effect of type of various desorption solvent for recovery of Ni^{2+}

Based on the results (Table 1), NaOH cannot be used as appropriate desorption and these bases do not possess a complete detergence power. Therefore, mineral acids with determined concentrations, H_2SO_4, and HNO_3 were applied. As shown in Table 1, the results of this table offer that all acids contain a good detergence power for Ni^{2+}, but the recovery percentage of HNO_3 is higher than that of other acids. In an acidic environment, the possible deposits dissolved and recovery of these ions increased. However, the results obtained from nitric acid were better than H_2SO_4, in that 0.1 M of solution washed 92.54% of the Ni^{2+} ion adsorbent. So, for the rest of the experiments, nitric acid 0.10 M was used as the desorption solution.

Survey of optimization of the volume effect of desorption solvent for Ni^{2+} recovery

After the investigation and choice of optimal desorption, the volume of solvent was investigated, with the results which are shown in Table 2. The volume of 12 mL for HNO_3 was selected as the optimal volume for washing.

Table 2

The optimum volume of the desorption solvent

Solvent volume	Recovery (%)
5 mL	43.29(0.3) [a]
7mL	58.4(0.5)
9 mL	75.69(0.6)
12 mL	90.79(0.8)
14 mL	86.14(0.2)
16mL	87.82(0.1)
18mL	87.95(0.5)

[a] Measurement RSD following three replications

Investigation the effect of breakthrough volume

Following the optimization of the pH of the desorption solvent and sample solution, etc., to elute the Ni^{2+} in the adsorbents, the maximum volume of the aqueous solution containing Ni^{2+} should be measured. If the volume of the test solution to be less than the breakthrough volume, and passaging of that volume, all analytes are kept in the solid phase. The results in (Table 3) verify that up to 250 mL of ions are adsorbed by the nano adsorbents and if the sample volume is greater than this value, some of the Ni^{2+} is not kept on the adsorbent and pass over the adsorbent with no inhibition. Also with definition by the concept of breakthrough volume, it can be reported that the breakthrough volume in the current study is 250 mL and if the sample solution volumes which includes Ni^{2+} is over 250 mL, adsorption does not occur completely and hence if 250 mL of sample volume is passed over the adsorbent and then with 12 mL of the desorption solvent washed, the concentration factor could not be achieved as 30. This concept that the concentration of Ni^{2+} in 7 mL of desorption solvent which was passed over the adsorbent grows by 20.8 times. Based on the related results (Table 3), the breakthrough volume calculations are as follows:

Table 3

Six investigations of the effect of solution volume in the sample

Recovery (%)	V(mL)
80.7(1.1) [a]	50
79.2(0.5)	100
78.7(0.5)	150
77.5(1.8)	250
65(1.6)	350
47(1.2)	500

[a] Measurement RSD following three replications

Concentration factor = breakthrough volume/the desorption solvent volume= 250/12=20.8.

Determination of the blank standard deviation (S_b)

The accuracy or replicability of any method is the main factor to recognize its validity and reliability. To inquire about the method's replicability, the results data of the study of four blank solutions (deionized water) deposited in Table 4.

Table 4

Measurement RSD following three replications

Device response	Sample
0.021(1.5) [a]	1
0.020(3.1)	2
0.021(1.5)	3
0.021(0.9)	4

[a] Measurement RSD following three replications

Based on the results achieved in Table 5, the blank standard deviation was obtained as follows; S_b=0.0004.

Determination of the accuracy and RSD% of the method

This parameter was used to investigate the accuracy and proximity of the examined data. As shown in Table 5, or the average of recoveries and S or standard deviation has been calculated for three tests and the relative standard deviation (RSD) achieved for three replications.

Table 5

Determination of %RSD of the method

Absorption	Sample
0.043(0.8)	1
0.042(0.9)	2
0.042(0.6)	3
0.043(0.6)	4

$\overline{X}$ =0.0425 S_b=0.00057

$$\%RSD = \frac{S}{\overline{X}} \times 100 = \frac{0.00057}{0.0425} \times 100 = 1.35\%$$

Table 6

The calibration curve for measurement of Ni^{2+}

Primary standard solution concentration µg. L^{-1}	Adsorption
20	0.05(3.6)
80	0.060(1.2)
200	0.098(1.5)
500	0.145(0.2)
800	0.302(0.4)

Table 7

The effect of interfering ions on the recovery of Ni^{2+}

Ions	Added value(ppm)	Recovery percentage Ni(II)
Na^+	200	85.12(1.5)[a]
Zn^{2+}	5.0	90.64(2.1)
K^+	200	86.58(1.6)
Mg^{2+}	100	86.58(1.6)
Cu^{2+}	5.0	89.43(1.2)
Cl^-	308.7	82.18(1.4)
NO_3^-	317	93.18(2.3)
SO_4^{2-}	400	92.94(1.6)

[a] Measurement RSD after three replications

The linear range and a calibration curve of the method

To assess the linear range in the analysis method, a calibration curve should be plotted. This curve is not linear across all concentrations and different factors cause the calibration curve to the situation in the linear range and follow from Beyer Law. Based on Table 7, the calibration curve of the method is as conform and the line equation is $y=0.002x+0.053$ and $R^2=0.99$.

Study of the effect of disturbances on the measurement of Ni^{2+}

A disturbing ion is an ion that causes a certain variation of over ±5% in the adsorption and recovery of Ni^{2+}. To study the effect of disturbance of other ions on Ni^{2+} extraction, a certain quantity of interfering factors added to the initial solution, and the experiment was performed at breakthrough volume. Absorption of the recovered solution is analyzed with flame atomic absorption and then compared versus the solution absorption resulting from the sample recovery which lacks the interfering ion. As can be shown in Table 7, in the presence of external ions, Ni recovery occurred with ±5% variations and the external ions had no particular effects on the analysis and cause no disturbance.

Determining the method's limit of detection

The lowest Ni^{2+} concentration or weight in a sample that could be determined with a certain confidence level is called the limit of detection

(LOD), which is defined as follows. The LOD of a method is a concentration of an analysis sample where the device response to concentration (which is significantly different from the response of the control sample) is defined as follows; the limit of detection is the lowest amount of Ni^{2+}, where the presented method can detect it. Based on the presented definition, LOD can be calculated by the following relation;

$$\mathrm{LOD} = \frac{3S_b}{m} \tag{11}$$

where S_b and m are the standard deviations of the blank signal and the slope of the calibration curve, respectively. Based on the experimented, S_b=0.0004 and the slope of the calibration curve is 0.0002.

Therefore, LOD can be calculated at 6.0 ppb.

Adsorption isotherms and kinetics

In this study, isotherms were surveyed by varying the concentration of Ni^{2+} ions solutions from 10 to 350 mg L^{-1} at pH 10 with a 0.05 g of the MWCNTs-COOH. The Langmuir, Freundlich, Temkin, Dubinin–Radushkevich isotherm models were applied to elucidate the adsorption mechanism. Table 8 summarizes all parameter values obtained from the isotherms used for the Ni^{2+} removal by the MWCNTs-COOH. The R^2 values were collected in Table 8 and shown in Figure 12 (b) revealed that Ni^{2+} adsorption experimental data by MWCNTs-COOH were fitted well with the Freundlich equation in the studied isotherms (R^2>0.98). This could be indicated by the multilayer adsorption by the MWCNTs-COOH. Moreover, the Langmuir model has larger R2 values after the Freundlich model to fitting experimental data of Ni^{2+} removal by MWCNTs-COOH. In this work, three kinetic models were employed to study the adsorption time and rate. For these intentions, the experiments were performed at optimum conditions at various time intervals up to 220 min. The equilibrium times were observed to be 180 min for adsorption of Ni^{2+} ions by, MWCNTs-COOH. As can be seen in Table 9, the R^2 values of the pseudo-second-order kinetic model are more than 0.99 for MWCNTs-COOH that shown in Figure 13 (b). So, the adsorption of Ni^{2+} ions by the MWCNTs-COOH can be revealed by the pseudo-second-order kinetic type and this model proposed that the rate in the adsorption process controlled by chemical adsorption mechanism.

Investigation of the obtained results on real sample

Once the optimum conditions of the method were achieved, to investigate the implementation ability of the method on real water samples, the level of Ni (II) was measured across different water and biological samples at 250 mL. In the first step, the sample itself was investigated without the addition of amounts of Ni^{2+} and it was also washed, and next it was injected into the apparatus. It was observed that the apparatus did not determine considerable absorption. In the second step, and by increasing the Ni^{2+}, it was carry outed according to the concentration and separation method. Actually, to determine certain amounts of Ni present in the samples, the standard elevation method was used. The results of this analysis are shown in Table 9. As can be seen, in the water samples, in the Tap water sample of Pishva–Varamin, on 27 Jan 2018, and industrial wastewater sample of Charmshar Varamin on 30 Jan 2018, there is a larger amount of Ni^{2+} than in the experimented water samples. Although, in other samples, there is less Ni. Based on this, the performance and power of preconcentration and Ni measurement could be deduced.

A comparison between the current method and other methods

A comparison of this method with other methods verified that the current method is more accurate, easiest, and faster as it had smaller relative standard deviation values in comparison with other methods.[29,45-53] The current method is one of the foremost systems for determining the very trace amounts of heavy metal ions including Ni in aqueous samples. Another point in the usage of nanotube adsorbent is that instead of using the proposed ligand, one can put other ligands on the adsorbent which to adsorb mineral ions, thereby measuring trace amounts of metal ions. A wide variety of ligands can be used given their properties, which act selective towards one or several ions and applying this set, preconcentration, and determination of cations can be carried out. Using flame atomic absorption and solid drop microextraction, single-drop liquid-liquid extraction, and homogeneous liquid-liquid extraction with other devices, one can determine trace amounts of Ni^{2+} by this adsorbent and achieve a smaller limit of detection value.

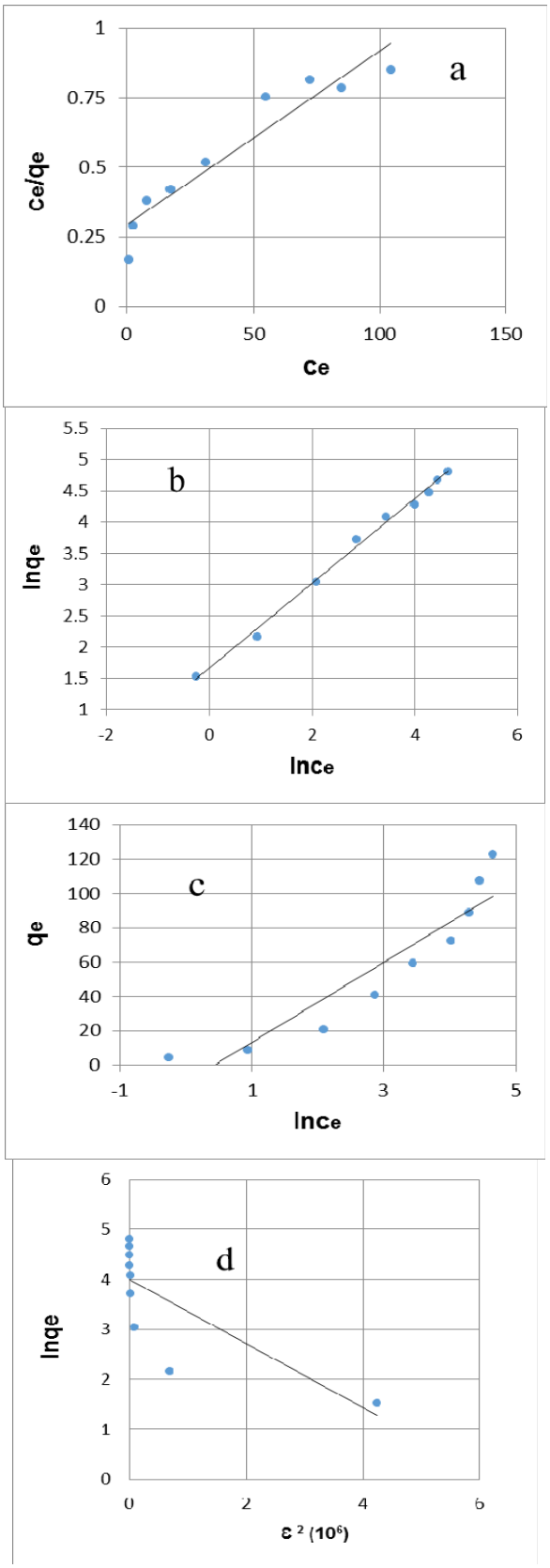

Fig. 12 – Linear isotherms models: a) Langmuir b) Freundlich c) Temkin
d) Dubinin-Radushkevich isotherm of Ni(II) on MWCNTs-COOH adsorbent.

Table 8

The results of Langmuir, Freundlich, Temkin and Dubunin-Radushkevich isotherm for adsorption of Ni(II) on MWCNTs-COOH adsorbent

Langmuir		Freundlich		Temkin		Dubinin–Radushkevich	
R^2	0.90	R^2	0.98	R^2	0.86	R^2	0.60
K_L ($L.mg^{-1}$)	0.02	K_F	5.24	A ($L.g^{-1}$)	0.65	E ($kJ.mol^{-1}$)	0.91
q_{max} ($mg.g^{-1}$)	158.73	1/n	0.67	B ($J.mol^{-1}$)	23.37	q_D ($mg.g^{-1}$)	54.82
R_L	0.82						

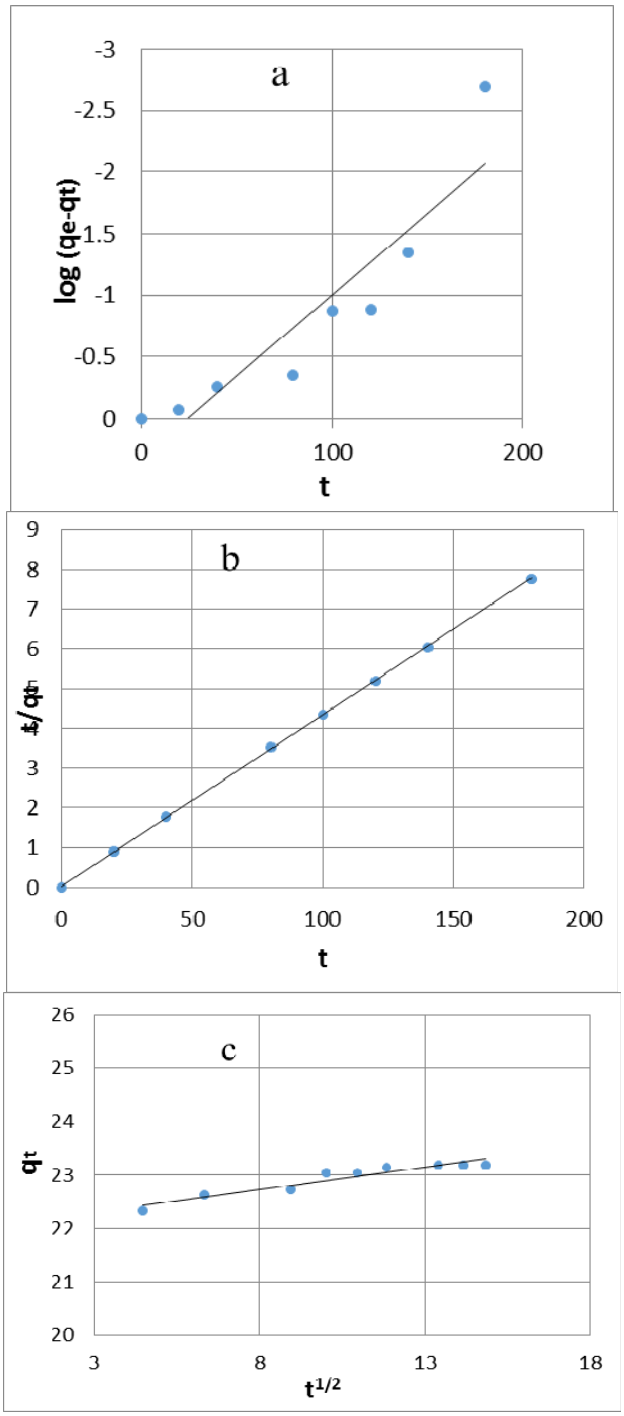

Fig. 13 – Linear kinetic plots for Ni (II) adsorption on MWCNTs-COOH adsorbent: a) pseudo-first-order, b) pseudo-second-order, c) intra-particle diffusion model.

Table 9

Pseudo-first order, Pseudo-second order, Intra-diffusion adsorption kinetic parameters

pseudo-first-order		pseudo-second-order		intraparticle diffusion	
k_1 / min^{-1}	0.0304	k_2 / g mg^{-1} min^{-1}	0.000103	K_P (mmol $g^{-1}min^{1/2}$)	0.09
q_e / mg g^{-1}	2.053525	q_e / mg g^{-1}	23.20	C	21.95
R^2	0.84	R^2	0.99	R^2	0.94

Table 10

The results of measurement of Ni in real samples

Ni (II) found in FAAS(μg)	Ni (II) added (μg)	**Sample**
N.D[b]	0.0	Well water of pishva
5.09(1.0)[a]	5.0	
0.067(1.9)	0.0	Tap Water of pishva
5.02(1.4)	5.0	
0.07(2.7)	0.0	Industrial wastewater Charmshar Varamin
5.02(1.8)	5.0	

[a)] Measurement% SD after three replications
[b)] Not Detection

CONCLUSIONS

In comparison with other procedures reported for measurement of Ni (II), this method has considerable advantages that are easy and inexpensive and can be applied quickly for environmental aqueous samples. Furthermore, it minimizes the utilization of organic, toxic, and costly solvents. Moreover, the design and development of this procedure for separation, measurement, and preconcentration of Ni^{2+} are essential considering its importance in various industries and the little concentration of Ni^{2+} ion in most samples. Therefore, this research aims to present an effective, selective, cost-effective, and simple method for measurement of the level of Ni (II) across different environmental aqueous samples (in this research, the limit of detection, the value of breakthrough volume, and RSD has been obtained). The adsorption isotherm results were more consistent with the Freundlich model. Also, the fitting of the kinetic results to the pseudo-second-order type demonstrates that Ni (II) chemisorbed in the rate-limiting step. This research indicated that the measurement of Ni^{2+} occurs at an appropriate level without the interference of any other interfering factor and thus the current method can be applied easily in the measurement of the quantity of Ni (II) in aqueous samples.

Acknowledgments. We gratefully acknowledge the financial of the department of chemistry, department of Varamin branch Islamic Azad University for financial support.

REFERENCES

1. S. Satarug, M. R. Haswell-Elkins and M. R. Moore, *British J. of Nutrition*, **2000**, *84*, 791.
2. A. Moghimi and M. Abniki, *Adv. J. of Chem.-Section A*, **2021**, *4*, 78.
3. M. A. Ganzoury, C. Chidiac, J. Kurtz and C.-F. de Lannoy, *J. of Hazardous Mater.*, **2020**, *393*, 122432.
4. M. N. Siddiqui, I. Ali, M. Asim and B. Chanbasha, *J. of Molec. Liq.*, **2020**, *308*, 113078.
5. S. Satarug, S. H. Garrett, M. A. Sens and D. A. Sens, *Environ. Health Perspectives*, **2010**, *118*, 182.
6. W. Jiang, J. Lv, L. Luo, K. Yang, Y. Lin, F. Hu, J. Zhang and S. Zhang, *J. of Hazardous Mater.*, **2013**, *262*, 55.
7. R. A. Vanderpool and W. T. Buckley, *Anal. Chem.*, **1999**, *71*, 652.
8. C. Kantar, *Rev. Roum. Chim.*, **2019**, *64*, 361.
9. A. Hachemaoui, *Rev. Roum. Chim.*, **2019**, *64*, 1097.
10. T. D. A. Maranhão, E. Martendal, D. L. Borges, E. Carasek, B. Welz and A. J. Curtius, *Spectrochim. Acta Part B: Atomic Spectroscopy*, **2007**, *62*, 1019.
11. Y. Liu, X. Chang, S. Wang, Y. Guo, B. Din and S. Meng, *Anal. Chim. Acta*, **2004**, *519*, 173.
12. L. Berthod, G. Roberts, D. C. Whitley, A. Sharpe and G. A. Mills, *Water Research*, **2014**, *67*, 292.
13. E. Bacalum, E.-E. Iorgulescu and V. David, *Rev. Roum. Chim.*, **2012**, *57*, 715.
14. S. Cerutti, M. Silva, J. Gasquez, R. Olsina and L. Martinez, *Spectrochim. Acta Part B: Atomic Spectroscopy*, **2003**, *58*, 43.
15. A. Moghimi, *Int. J. Bio-Inorg. Hybr. Nanomater*, **2016**, *5*, 203.

16. A. Ceccarini, I. Cecchini and R. Fuoco, *Microchem. J.*, **2005**, *79*, 21.
17. T. Pourshamsi, F. Amri and M. Abniki, *J. of the Iran. Chem. Soc.*, **2020**, 1.
18. A. Moghimi and M. Abdouss, *Int. J. Bio.-Inorg. Hybd. Nanomat.*, **2013**, *2*, 319.
19. A. Moghimi, M. Saber-Tehrani, S. Waqif-Husain and M. Mohammadhosseini, *Chinese J. of Chem.*, **2007**, *25*, 1859.
20. G. D. Tarigh and F. Shemirani, *Talanta*, **2013**, *115*, 744.
21. A. Moghimi and M. J. Poursharifi, *Oriental J. of Chem.*, **2012**, *28*, 353.
22. A. Moghimi, *Russ. J. of Phys. Chem. A*, **2014**, *88*, 2157.
23. A. Moghimi, M. Qomi, M. Yari and M. Abniki, *Int. J. Bio-Inorg. Hybr.* Nanomater, **2019,** *8,* 163-172
24. A. Moghimi and M. Yari, *Merit Research J. of Environ. Sci. and Toxicol.*, **2014**, *2*, 110.
25. A. Moghimi and S. P. Akbarieh, *Int. J. of Sci. Research in Knowledge*, **2014**, *2*, 8.
26. A. Moghimi, *Russ. J. of Phys. Chem. A*, **2013**, *87*, 1203.
27. M. Abniki and A. Moghimi, *Micro & Nano Letters*, **2021,** *16,* 455-462
28. A. Moghimi, M. Abdouss and G. Ghooshchi, *Int. J. Bio.-Inorg. Hybd. Nanomat.*, **2013**, *2*, 355.
29. A. Moghimi and M. Shabanzadeh, *J. of Chem. Health Risks*, **2012**, *2*, 7-16
30. P. Thistlethwaite and M. Hook, *Langmuir*, **2000**, *16*, 4993.
31. A. Moghimi and M. Abniki, *Chem. Method.*, **2021**, *5*, 250.
32. Y. A. El-Reash, *J. of Environ. Chem. Eng.*, **2016**, *4*, 3835.
33. U. Shafique, A. Ijaz, M. Salman, W. Uz Zaman, N. Jamil, R. Rehman and A. Javaid, *J. of the Taiwan Institute of Chem. Eng.*, **2012**, *43*, 256.
34. M. Abniki, Z. Azizi and H. A. Panahi, *IET Nanobiotechnol.*, **2021**, *15,* 664-673.
35. A. Maleki, E. Pajootan and B. Hayati, *J. of the Taiwan Institute of Chem. Engs.*, **2015**, *51*, 127.
36. S. Ghanavati Nasab, A. Teimouri, M. Hemmasi, Z. Jafari Harandi and M. Javaheran Yazd, *Int. J. of Environ. Anal. Chem.*, **2020**;10.1080/03067319.2019.16999171-22.
37. K. Y. Foo and B. H. Hameed, *Chem. Eng. J.*, **2010**, *156*, 2.
38. S. Lagergren, S. Lagergren, S. Lagergren and K. Sven, **1898**, *24,* 1-39.
39. H. Ys, G. Mckay, H. Ys and G. Mckay, *Process Biochem.*, **1999**, *34*, 451.
40. W. J. Weber and J. C. Morris, *J. of the Sanitary Eng. Division*, **1963**, *89*, 31.
41. M. Abniki, A. Moghimi and F. Azizinejad, *J. of the Serbian Chem. Soc.*, **2020**, *85*, 1223.
42. M. Abniki, A. Moghimi and F. Azizinejad, *J of the Chinese Chem. Soc.*, **2021**, *68*, 343.
43. A. Moghimi and M. Abniki, *J. of Color Sci. and Technol.*, **2021**, *No volume and page (first accept)*
44. J. D. Patel, T. T. D. Vu and F. Mighri, *Mater. Lett.*, **2017**, *196*, 161.
45. F. Xie, X. Lin, X. Wu and Z. Xie, *Talanta*, **2008**, *74*, 836.
46. A. Goswami, A. K. Singh and B. Venkataramani, *Talanta*, **2003**, *60*, 1141.
47. A. Moghimi, *Australian J. of Basic and Appl. Sci.*, **2012**, *6*, 320.
48. M. Ali, *Chinese J. of Chem.*, **2007**, *25*, 640.
49. M. Herrera-Alonso, A. A. Abdala, M. J. McAllister, I. A. Aksay and R. K. Prud'homme, *Langmuir*, **2007**, *23*, 10644.
50. A. Anumah, H. Louis, S.-U. Zafar, A. T. Hamzat, O. O. Amusan, A. I. Pigweh, O. U. Akakuru, A. T. Adeleye and T. O. Magu, *Asian J. of Green Chem.*, **2019**, *3*, 283.
51. F. K Behbahani and R. Shahbazi, *Chem. Methodologies*, **2018**, *2*, 270.
52. A. Moghimi, *Integrated J. of British*, **2014**, *1*, 11.
53. M. Ghaedi, M. Reza Fathi, A. Shokrollahi and F. Shajarat, *Anal. Lett.*, **2006**, *39*, 1171.